Journal of Medicinal Chemistry

Article

Inclusion of a Photosensitizer in Liposomes Formed by DMPC/Gemini Surfactant: Correlation between Physicochemical and Biological Features of the Complexes

Cecilia Bombelli, Giulio Caracciolo, Pietro Di Profio, Marco Diociaiuti, Paola Luciani, Giovanna Mancini, Claudia Mazzuca, Manuela Marra, Agnese Molinari, Donato Monti, Laura Toccacieli, and Mariano Venanzi

J. Med. Chem., **2005**, 48 (15), 4882-4891• DOI: 10.1021/jm050182d • Publication Date (Web): 28 June 2005

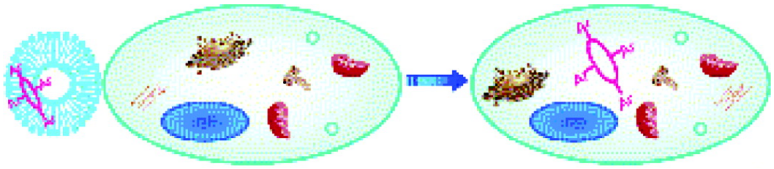

Inclusion of a Photosensitizer in Liposomes Formed by DMPC/Gemini Surfactant: Correlation between Physicochemical and Biological Features of the Complexes

Cecilia Bombelli,[†,‡] Giulio Caracciolo,[§] Pietro Di Profio,[‡,∥] Marco Diociaiuti,[⊥] Paola Luciani,[†,‡] Giovanna Mancini,[*,†,‡] Claudia Mazzuca,[#] Manuela Marra,[⊥] Agnese Molinari,[⊥] Donato Monti,[#] Laura Toccacieli,[⊥] and Mariano Venanzi[#]

CNR Istituto di Metodologie Chimiche-Sezione Meccanismi di Reazione, and Dipartimento di Chimica, Università degli Studi di Roma "La Sapienza", P.le A. Moro 5, I-00185 Roma, Italy; Centro di Eccellenza per i Materiali Innovativi Nanostrutturati per Applicazioni Chimiche, Fisiche e Biomediche, CEMIN; Dipartimento di Chimica, Università di Perugia, Via Elce di Sotto 8, Perugia, 06123, Italy; Dipartimento di Tecnologie e Salute, Istituto Superiore di Sanità, V.le Regina Elena 299, 00161 Roma, Italy; and Dipartimento di Scienze e Tecnologie Chimiche, Università degli Studi di Roma "Tor Vergata", Via della Ricerca Scientifica 1, I-00133 Roma, Italy

Received February 25, 2005

Mixed cationic liposomes composed by different ratios of dimyristoyl-*sn-glycero*-phosphatidylcoline (DMPC) and a cationic gemini surfactant have been studied by various physicochemical tools as vehicles for *m*-tetrahydroxyphenylchlorin (*m*-THPC), a photosensitizer used in photodynamic therapy. Entrapment and location of *m*-THPC within the lipid double layer have been evaluated by different techniques and the new formulations have been tested on a stabilized cell line from a human colon tumor, COLO206. A correlation between the physicochemical features of formulations and their efficiency as photosensitizers vector was found.

1. Introduction

Since their description in 1965,[1] liposomes have been attracting attention as potential carriers for a variety of drugs, including traditional ones, proteins, hormones and diagnostic agents. Liposomes have been shown to be effective in delivering many therapeutic agents to cells and tissues[2] and feature many advantages compared with other drug delivery systems (DDS). Their relative ease of preparation, biocompatibility and biodegradability, broad selection and control of their properties, potential for high drug loading efficiency, and partial intrinsic selectivity (it is indeed well-known that liposomes do not accumulate in some organs such as heart and kidneys[3]) are, in fact, their main advantages, in contrast with some stability problems, concerning both the encapsulated drug and the phospholipids bilayer.

A therapeutic treatment in which liposome formulations have been tested successfully is photodynamic therapy (PDT); in fact, many porphirins[4] and related systems, the most important class of photosensitizers (PS) used in PDT, can be efficiently and stably dissolved in the liposome bilayer. The intrinsic efficacy and safety of PDT can be improved by using liposome formulations: studies performed on different tumor models have shown, in fact, that liposomes provide a heightened tumor accumulation of PS.[5] Moreover, most photosensitizers are hydrophobic and in aqueous media give rise to aggregation that significantly reduces PS efficacy;[6] liposome formulations decrease the extent of this aggregation, increasing PS photoactive population;[7] finally, liposomes can also affect the pharmacokinetic and the subcellular fate of the PS.[8]

Commercial liposomes formulations are made essentially of natural phospholipids; several formulations that include synthetic additives are used in PDT preclinical trials[9] in order to fulfill unmet, or partially unmet, goals of these lipidic delivery systems: increase of absorption, improvement of controlled release and, most importantly, target specificity with the consequent reduction of the systemic photosensibilization. Liposomes composed by natural phospholipids and cationic lipids or surfactants are used, with good results, in delivering DNA or RNA to cells,[10] but their potential for drug delivery is not much investigated; conversely, the possibility of an overall cationic charge on the liposome surface could be advantageous in a wide range of situations,[11] first of all in preventing liposome aggregation. Among cationic additives, a unique class is represented by cationic "gemini" surfactants;[12] these amphiphiles contain two polar heads, linked by a spacer, and two aliphatic chains. It has recently been shown that this kind of molecules can display higher transfection activities as compared to traditional cationic surfactants;[13] moreover, the addition of gemini surfactants to natural phospholipid liposomes is the more recent approach[14] to solve a limiting problem concerning the practical use of liposomes as DDS, that is, the leakage of entrapped materials during storage. Gemini can, in fact, contribute to strengthening the liposome bilayer,

* Corresponding author. Tel.: +390649913078. Fax: +3906490421. E-mail: giovanna.mancini@uniroma1.it.
† CNR Istituto di Metodologie Chimiche-Sezione Meccanismi di Reazione and Dipartimento di Chimica, Università degli Studi di Roma "La Sapienza".
‡ CEMIN.
§ Dipartimento di Chimica, Università degli Studi di Roma "La Sapienza".
∥ Università di Perugia
⊥ Istituto Superiore di Sanità.
Università degli Studi di Roma "Tor Vergata".

10.1021/jm050182d CCC: $30.25
Published on Web 06/28/2005

Chart 1. Natural Phospholipids (DMPC) and the Synthetic Gemini Surfactant (1) Used for Liposomes Preparation and the Second-Generation Photosensitizer (*m*-THPC)

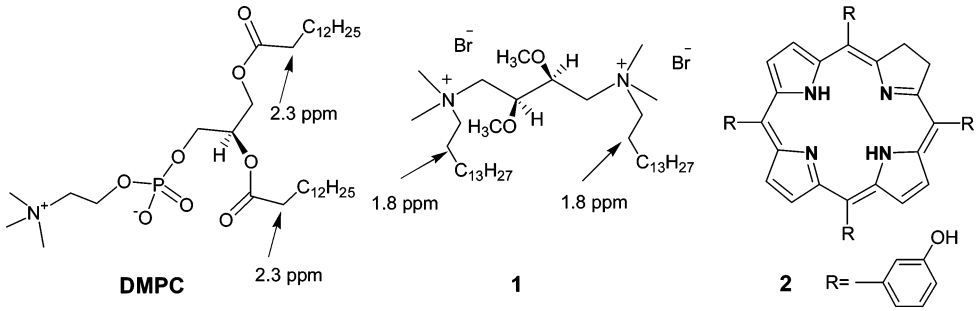

because their hydrophobic chains are characterized by a closer packing[12] with respect to single chain amphiphiles.

Here we report an investigation on mixed binary systems, composed by different percentages of DMPC and of the synthetic gemini surfactant **1**, in the presence and in the absence of *m*-THPC (*m*-tetrahydroxyphenylchlorin) **2** (Chart 1), a second-generation photosensitizer used in preclinical trials involving PDT. It has been tested for PDT of early cancers in the upper aereodigestive tract, tracheobronchial tree, and esophagus.[15] It features several advantages over Photophrin, among which are high purity, strong absorption in the NIR region, good selectivity for cancerous tissues,[16] and low skin sensitizing activity.[17] We choose *m*-THPC for this investigation in virtue of its definite structure, as opposed to Photophrin, and because of the symmetry of its molecular structure. The choice of a symmetric molecule rules out the occurrence of effects arising from an asymmetric substitution pattern on the periphery of the macrocycle.

Despite the large number of investigations in the field of DDS, very little attention is paid, as far as we know, to a relationship between, on one hand, entrapment ability and delivering efficiency and, on the other, the structural and physicochemical features of the carrier. We believe that the possibility of correlating the morphological and physicochemical features of the carriers with their biological features is crucial for a rational and systematic approach in designing new carriers for drug delivery. Here we report the physicochemical characterization of the aggregates, with particular attention to the effect of the gemini surfactant on liposome properties (structure and dimensions, membrane transition temperature, entrapment ability, localization of the drug in the bilayer), and the results of in vitro uptake experiments on a stabilized cell line from a human colon tumor, COLO206,[18] with the aim of correlating the composition and structure of the vehicle and the efficiency of delivery.

2. Results and Discussion

2.1. Effect of Cationic Gemini 1 on *m*-THPC Entrapment in DMPC/1 Liposomes. Gel filtration of extruded DMPC/**1** liposomes containing *m*-THPC allowed us to separate the unentrapped chlorin (i.e. chlorin in the buffer) from that entrapped in the lipid double layer. The determination of the percentage of entrapped chlorin, according to eq 2, requires as an internal check the measurement of the total lipid amount before and after gel filtration. These measurements were made by collecting ^{1}H NMR spectra of the CD_3OD solutions of the previously dried liposomes suspensions, in the presence of an internal standard. From these measurements the loss in total lipids was $\leq$1% for all the examined formulations. In Table 1 we reported the results of drug entrapment efficiency experiments in DMPC/**1** liposomes.

Table 1. Entrapped *m*-THPC in Liposome Formulations

DMPC (molar %)	**1** (molar%)	% *m*-THPC[a]
100	0	95
80	20	85
70	30	70
60	40	65

[a] Percentages with respect to the analytical concentration of chlorin in the mixed film (see section 4.3). Error in the determinations is 5%.

The percentage of entrapped chlorin decreases by increasing the percentage of **1** in the liposome formulations. This unexpected result[14] indicates that, in this case, the closer packing of gemini hydrophobic chains is less important than other interactions in the formation of the aggregates.

2.2. Effect of Cationic Gemini 1 on DMPC Double Layer Transition Temperature. The emission spectrum by Laurdan bound to a membrane in the gel state shows one peak at 450 nm, whereas the spectrum of Laurdan in a membrane in the liquid crystalline state shows a peak at 490 nm; in the range of coexistence of the two phases, the Laurdan spectrum shows a peak at intermediate wavelengths.

The transition temperature was measured only for mixed liposome formulations up to a molar ratio DMPC/**1** 6:4 because higher percentages of gemini yield gel solutions.

Laurdan emission spectra were acquired for DMPC/**1** vesicles in a range of temperatures spanning the bilayer phase transition of DMPC (297.3 K). For each liposome formulation the steady-state G_p values were calculated from the spectra as described in section 2.6 and plotted as a function of temperature (Figure 1). Inflection point in the plots represent the transition temperature of each formulation (these were more clearly evidenced by the break in the plot of $\Delta G_p/\Delta T$ versus ΔT). It can be observed that the inflection point is less pronounced at increasing percentage of gemini. This demonstrates a progressive insensitivity of membrane to the change of temperature; a similar effect was reported for the addition of cholesterol to vesicles formed by natural phospholipids.[19]

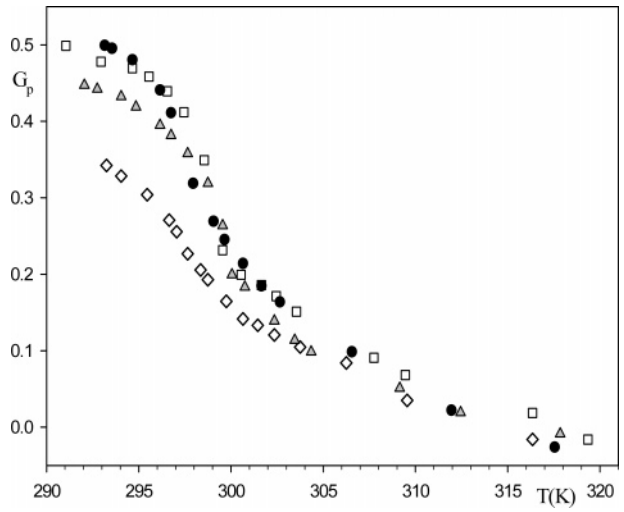

Figure 1. Spectrofluorimetric determination of mixed liposomes transition temperature. G_p versus T is reported. The inflection point in each plot corresponds to the transition temperature: T (K) DMPC = 297.3; T (K) DMPC/**1** 8:2 = 290.0; T (K) DMPC/**1** 7:3 = 299.9; T (K) DMPC/**1** 6:4 = 297.3.

The transition temperature increases linearly up to 30% of gemini surfactant in the formulation, with an increase of 2.5 K as compared with pure DMPC, whereas it decreases in the formulation containing 40% of **1**. This break in the correlation between composition/transition temperature may suggest a phase transition.

2.3. Morphological Analysis by Transmission Electron Microscopy (TEM). Morphological analysis by transmission electron microscopy were carried out on the liposome dispersions up to a 5/5 DMPC/**1** molar ratio, in the presence and in the absence of chlorin. Samples were analyzed by the contrast method. The negative staining of samples was obtained with a 2% w/v solution of phosphotungstate acid buffered at pH = 7.4. The heavy metal (W) surrounding the particle scatters electrons more efficiently than the particle itself, providing enough image contrast and allowing a detailed examination of the structure. Moreover, heavy metal salts give good radiation protection and maintain the specimen integrity. The attainable resolution can be evaluated on the order of 2 nm.[20]

In Figure 2a an image of pure DMPC liposomes is reported. The images relative to dispersions containing pure DMPC show a unilamellar vesicle, with a diameter of 80 nm, and some more complex structures, resulting from stacking of several double layers. The images relative to liposomes containing up to 30% of the gemini surfactant (Figure 2b,c), in the presence and in the absence of *m*-THPC, show fused, nonspherical, multilamellar structures without an aqueous internal phase. Multilamellarity is observed despite using a liposome preparation procedure that generally yields unilamellar vesicles. The images of formulations containing more than 40% of gemini surfactant (Figure 2d) show fibers and structures similar to crystals (all formulations containing more than 50% of **1** are gels at room temperature).

2.4. Morphological Analysis by Dynamic Light Scattering (DLS). All measurements were made at 2.5 mM DMPC in 0.1 M NaCl. It is apparent from Table 2 that DMPC:**1** at a ratio down to 7:3 shows the expected monodisperse population, whereas (Table 3) at 6:4, a striking increase of dimensions is observed. In the latter case, a larger sized, minor population is observed around 600 nm, which is quite above the Rayleigh scattering region,[21] and this value can only be considered as an indication for the formation of large anisotropic structures beyond 150 nm. DLS measurements show, analogously to the measurements of fluorescence and TEM, a change in the physicochemical and morphological features of the aggregates for the formulation containing 40% of **1**.

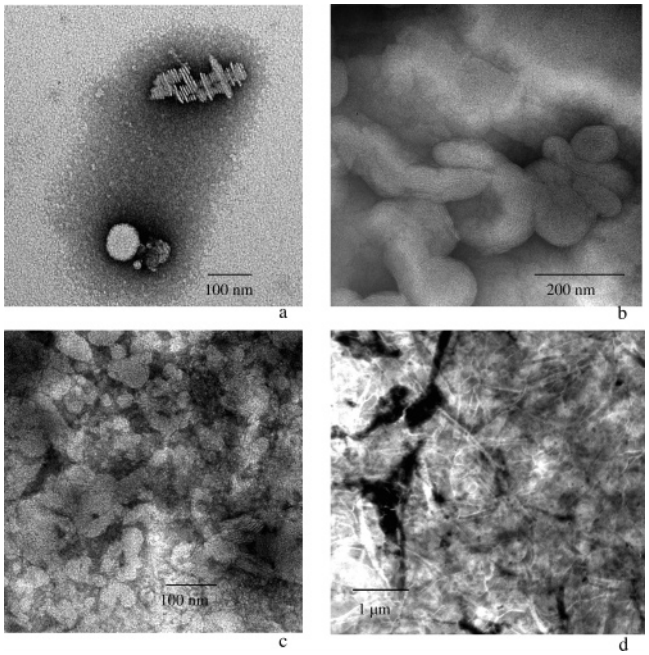

Figure 2. TEM images of liposomes formulations: (a) pure DMPC liposomes, (b) DMPC/**1** 8:2 liposomes, (c) DMPC/**1** liposomes 7:3 containing *m*-THPC, (d) formulation DMPC/**1** 5:5 containing *m*-THPC.

Table 2. Size of Liposomes Containing up to 30% of 1 Obtained by DLS[a]

DMPC:1 ratio	intensity-weighted diameter (nm)	χ^2	coefficient of variation (%)
10:0	103	0.43	22
8:2	112	0.52	23
7:3	109	0.23	20

[a] Monodisperse populations according to cumulants analysis.[32]

Table 3. Size of Liposomes Containing 40% of 1 Obtained by DLS[a]

	intensity-weighted diameter (nm)			
DMPC:1 ratio	major population[b]	minor population[c]	fit error[d]	residual[d]
6:4	150	600	1.10	0.0

[a] Bimodal population according to ILT.[33] [b] Population contributing ca. 40% of light scattered, equivalent to ca. 98% of particles in number. [c] Population contributing ca. 57% of light scattered, equivalent to ca. 1% of particles in number. [d] Fit error and residual represent goodness-of-fit values for a NLLS fit (ILT[a]).

2.5. Fluorescence Experiments. Steady-state and time-resolved fluorescence measurements were performed on *m*-THPC entrapped in DMPC and in DMPC/**1** dispersions (8/2, 7/3, 6/4). As can be evinced by the experimental data reported in Table 4, the emission spectral features of *m*-THPC are not affected by the inclusion in the different liposome formulations.

Table 4. Emission Maximum (λ), Time Decay (τ), and Anisotropy Coefficient (r) of *m*-THPC in Ethanol and in Liposome Formulations

phase	λ (nm)	τ (ns)	r
ethanol	649	9.1	0.02
DMPC	650	9.3	0.11
DMPC/**1** 8/2	651	9.0	0.12
DMPC/**1** 7/3	651	2.8 (0.11), 8.6 (0.89)	0.11
DMPC/**1** 6/4	649	4.5 (0.37), 9.4 (0.63)	nd

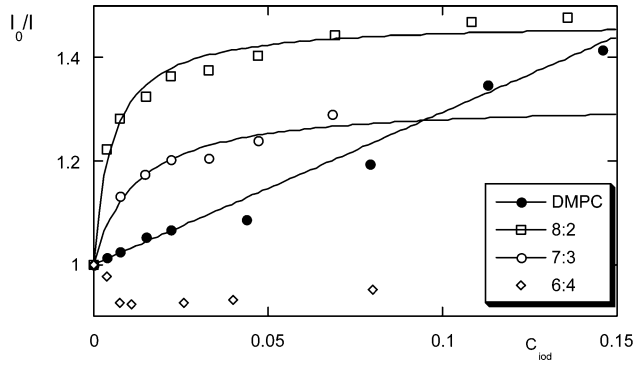

Figure 3. Fluorescence quenching experiments of *m*-THPC in liposome formulations by iodide.

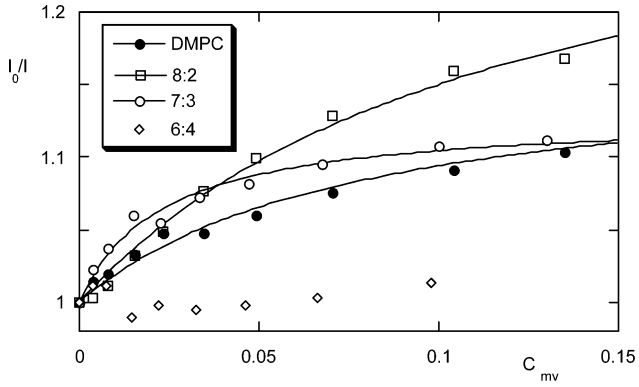

Figure 4. Fluorescence quenching experiments of *m*-THPC in liposome formulations by methyl viologen.

The emission time decays of *m*-THPC in DMPC and DMPC/**1** 8:2 are strictly monoexponential, with a lifetime similar to that measured in ethanol solution and typical of the emission of chlorin monomeric forms. On the contrary, *m*-THPC in DMPC/**1** 7:3 and 6:4 showed a two time component decay, with the shorter lifetime having relative weights increasing with the fraction of gemini surfactant. Anisotropy measurements reveal that the *m*-THPC molecules are well-embedded in the liposome phase, the anisotropy coefficient reaching, in all the liposome formulations, the limit r_0 value.[22] Fluorescent quenching experiments on *m*-THPC in DMPC and DMPC/**1** surfactant formulations (8/2, 7/3, 6/4) were performed by using iodide (I^-) and methyl viologen (MV^{2+}) as collisional quenchers.

Experimental results are reported in Figure 3 for I^- and Figure 4 for MV^{2+} titration, respectively. The linear dependence from the I^- concentration measured for *m*-THPC in DMPC indicates that the chlorin molecule can be approached by the quencher at very short distances, suggesting a location of the fluorescent probe proximal to the liposome surface. By adding the surfactant component to DMPC, the fluorescence quenching behavior notably changes. The data can be described in terms of two different populations of the fluorophore: the first corresponds to the fraction (f) of molecules readily accessible to the quencher molecule, showing a characteristic quenching constant K, and the latter to the fraction $(1 - f)$ that cannot be approached by the quencher, i.e.,

$$\frac{I}{I_0} = (1 - f) + \frac{f}{1 + K[Q]} \qquad (1)$$

By applying eq 1 to the steady-state fluorecence quenching experiments we found $f = 0.33$ ($K = 277\ M^{-1}$) for *m*-THPC in DMPC/**1** 8:2 and $f = 0.25$ ($K = 66\ M^{-1}$) for *m*-THPC in DMPC/**1** 7:3. The quenching constant K measures the stability of the quencher−probe complex and is related to the separation distance within the excited-state complex. This model was confirmed by time-resolved fluorescence quenching measurements that reveal the presence of two different populations of fluorophores, the first characterized by a shorter time, corresponding to the quenched molecules, and the second fraction showing the same lifetime as unperturbed molecules. From time-resolved quenching experiments we obtained $f = 0.35$ for *m*-THPC in DMPC/**1** 8:2 and $f = 0.33$ for *m*-THPC in DMPC/**1** 7:3. On the contrary, *m*-THPC in DMPC/**1** 6:4 is not affected by addition of I^-, indicating that the fluorescent probe is located in a position inaccessible to the quencher molecule.

Quite the same results are obtained by using MV^{2+} as quencher (Figure 4). The cationic nature of the quencher, however, discourages its approach to the fluorescent probe hosted in the cationic liposome/gemini surfactant formulation. As a result, a minor quenching constant and lower fractions of accessible fluorescent molecules are measured. We obtained $f = 0.25$ ($K = 11\ M^{-1}$) for *m*-THPC in DMPC/**1** 8:2 and $f = 0.11$ ($K = 47\ M^{-1}$) for *m*-THPC in DMPC/**1** 7:3. Even *m*-THPC in DMPC shows a minor fraction of molecules quenched by MV^{2+} ($f = 0.14$, $K = 11\ M^{-1}$). The substantial insensitivity of *m*-THPC in DMPC/**1** 6:4 to quencher molecules is confirmed by MV^{2+} quenching experiments, as can be easily seen from Figure 4.

In summary, fluorescence experiments indicate that *m*-THPC is well-embedded in all the liposome formulations here investigated. By addition of surfactant molecules, a partition of the fluorescent probe in two different domains is revealed by fluorescence-quenching experiments using both anionic and (less efficiently) cationic quenchers. At high surfactant content, a structural transition of the liposome phase probably occurs, excluding the chlorin molecule from the collisional radius of the quencher molecules. This finding could be explained in terms of the deep location of the PS within the liposome multilayer or a gelification of the liposome phase that inhibits the diffusion of the quencher to the fluorescent molecule.

2.6. EDXD Experiments. The structural changes induced on DMPC bilayer by the addition of the cationic gemini surfactant **1** were investigated as a function of the lipid-to-surfactant molar ratio. The EDXD pattern of DMPC/**1** at a molar ratio 8:2 (Figure 5, full circles) shows two Bragg peaks (00l), positioned at $q = 0.105$

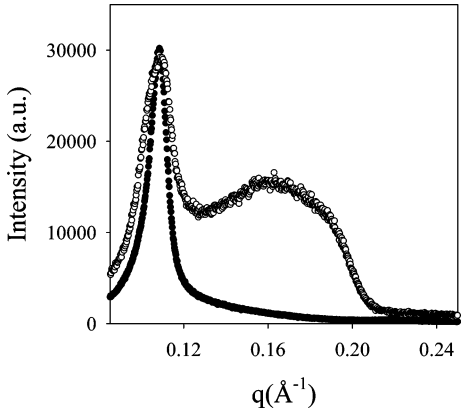

Figure 5. Comparison between the EDXD patterns of DMPC:**1** at a molar ratio 8:2 (full circles) and 6:4 (open circles), respectively. At a 8:2 molar ratio, the structure of the sample resembles that of pure lamellar DMPC while, at a 6:4 molar ratio, a new emerging phase appears.

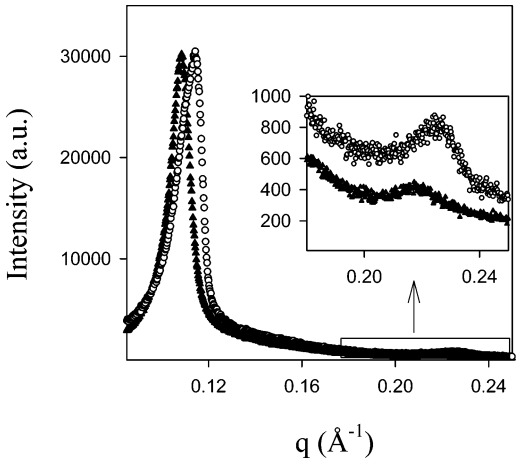

Figure 6. EDXD patterns of DMPC:**1** 8:2 with encapsulated *m*-THPC (open circles) and with no encapsulated material (full triangles).

and 0.210 Å^{-1}. Thus, the scattering distribution indicates a well-ordered lamellar structure of stacked membranes with a periodicity d of 59.8 Å ($d = 2\pi/q_{001}$). This value is shorter than that usually observed in fully hydrated DMPC multibilayers and this effect is due to the partly dehydration of the samples, which reduces the number of water molecules per lipid molecule and, consequently, the thickness of the water layer between opposing DMPC membranes, as elsewhere discussed.[23]

DMPC/**1** mixture containing surfactant-to-lipid molar ratio 7:3 (data not reported) shows the presence of the liquid-crystalline phase of DMPC with no appreciable difference in the lattice d-spacing. Conversely, at a molar ratio 6:4, remarkable changes in the lipid/surfactant system are produced and it unmistakably presents a peculiar behavior. In fact, even if the first-order Bragg peak of DMPC still remains present (Figure 5, open circles), a new phase appears. In the EDXD pattern a growing broad peak is evident. The exact nature of this emerging phase has been elucidated by EDXD experiments at a higher percentage of surfactant, and a detailed description will be given elsewhere. However, the observed changes in the diffraction pattern can be imputable to the solubilization of DMPC membranes operated by **1** molecules that start to solubilize the lipid lamellar structure.

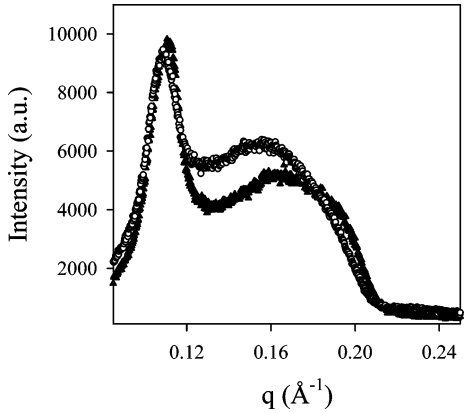

Figure 7. EDXD patterns of DMPC:**1** 6:4 with encapsulated *m*-THPC (open circles) and with no encapsulated material (full triangles).

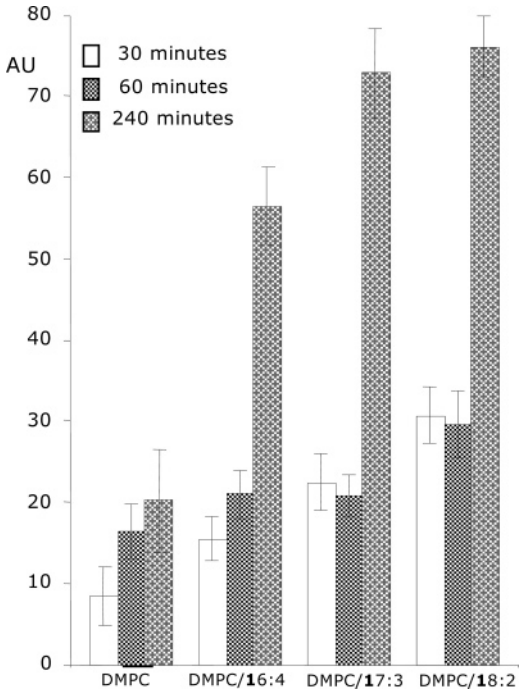

Figure 8. Cellular distribution of *m*-THPC in liposome formulations analyzed by flow cytometry. Efficiency of delivery at different times for liposome formulations are reported.

Further EDXD experiments on DMPC/**1** mixtures containing *m*-THPC were carried out in order to get insight on the exact location of the chlorin with respect to the DMPC bilayer surface. It is well-known that the membrane affinity of a photosensitizer is governed by its amphiphilic character, which is dependent on the arrangement of hydrophobic and hydrophilic substituents in the structure.[24] This arrangement modulates the ability of a photosensitizer to localize at the hydrophilic/hydrophobic interfaces of membranes. The structure of DMPC/**1** vesicles with entrapped chlorin molecules was characterized and compared to the experimental control consisting of pure vesicles with no entrapped PS.

Up to 7:3 ratio, the main effect of *m*-THPC on the lamellar structure of DMPC is a reduction of the lamellar periodicity d. More in detail, the first-order Bragg peak shifts from 0.105 to 0.111 Å^{-1} with a reduction of the lamellar d-spacing of about 2 Å. The interpretation of the observed phenomenon is 2-fold. The

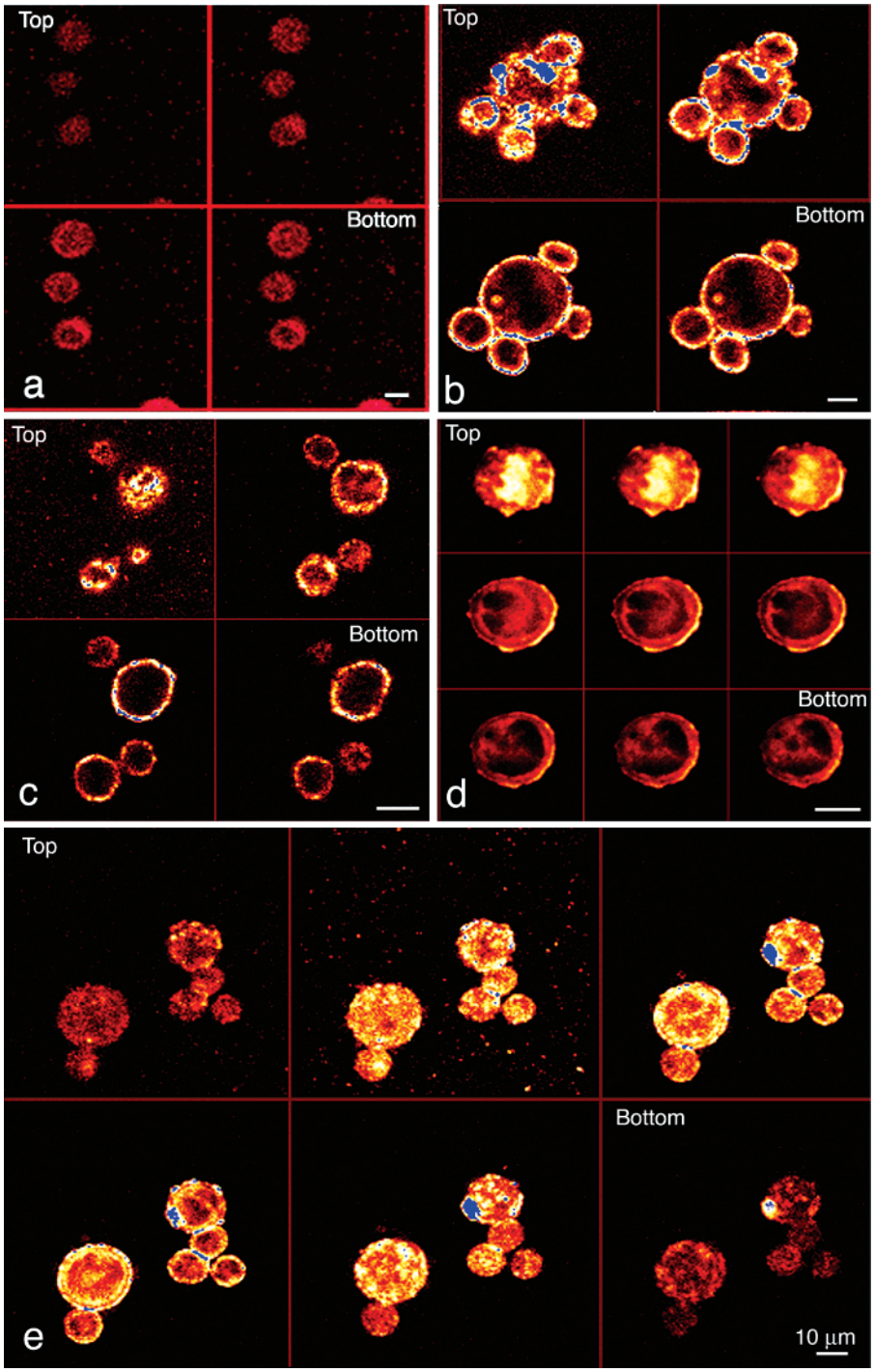

Figure 9. Cellular distribution of *m*-THPC in liposome formulations analyzed by laser scanning confocal microscopy (LSCM). The fluorescence dispayed by *m*-THPC carried by different liposome formulations in cells is reported: (a) DMPC vesicles after 1 h (very low); (b) DMPC/**1** 7:3 vesicles after 1 h (strong fluorescence in the plasma membrane); (c) DMPC/**1** 8:2 vesicles after 1 h (strong fluorescence in the plasma membrane); (d) DMPC/**1** 7:3 vesicles after 4 h (fluorescence in the cytoplasm and in the nuclei); (e) DMPC/**1** 8:2 vesicles after 4 h (strong fluorescence in the cytoplasm and in the nuclei).

interaction, at the bilayer surface, between the aromatic system of *m*-THPC and the ammonium groups of the amphiphiles could screen the repulsion between opposing lipid membranes, thus reducing the lamellar periodicity *d*. This interaction also reduces the lipid level of hydration, i.e., the number of water molecules per lipid molecule, thus reducing the thickness of the water layer between adjacent bilayers. Additionally, we observe a pronounced increase in the second-order reflection intensity in the EDXD pattern of DMPC/**1** with entrapped *m*-THPC (Figure 6, inset).

We propose that this effect depends on the reduced thickness of the water layer between adjacent bilayers. In the inset of Figure 6, second-order Bragg reflections are visible. Since diffraction peaks represent interbilayer coherence, the main effect of *m*-THPC on the lamellar structure appears to be a progressive stabilization of the multibilayer structure of DMPC and a reduction of the "second-order disorder" in the crystal lattice.

At a 6:4 ratio, the effect of *m*-THPC on the inner structure of DMPC/**1** vesicles is opposite with respect

to that observed in the 8:2 and 7:3 samples. In Figure 7, a direct comparison between the EDXD patterns of DMPC:**1** 6:4 with *m*-THPC (open circles) and with no encapsulated material (full triangles) is reported. The main effect is a plain increase of the lamellar *d*-spacing up to ~61 Å. This trend was experimentally verified by other investigators as a function of increasing surfactant-to-lipid ratio.[25] It is accepted that lamellar periodicity increases after chlorin is encapsulated, simply because the chlorin molecules are enclosed within the hydrophobic region of the vesicles, causing the bilayer membrane to enlarge.[26]

In conclusion, our EDXD experiments have shown that the fluidity of the liposome membrane changes as a function of the surfactant-to-lipid molar ratio and this is responsible for the location of the chlorin with respect to the DMPC bilayer surface. As a consequence, at lipid-to-surfactant ratios >6:4 the photosensitizer strongly interacts with the lipid headgroups at the membrane interface, reducing the interbilayer repulsion and the lamellar periodicity *d*. At a 6:4 ratio, the lamellar structure of DMPC changes, allowing the chlorin to penetrate in the hydrophobic region of the membranes. Indeed, at lipid-to-surfactant ratios ≤6:4 the latter EDXD experiments (Figure 3) confirm the accepted viewpoint that fluidizing the membrane by increasing the surfactant percentage pushes the photosensitizer deeper into the membrane and enlarges the thickness of the membrane and, in turn, of the lamellar periodicity *d*.[24]

2.7. Interaction of Different Liposome Formulations with Cells. To study the influence of gemini **1** on the interaction of liposomes/*m*-THPC formulations with cells, the accumulation and cellular distribution of the photosensitizer was analyzed by flow cytometry and laser scanning confocal microscopy (LSCM), respectively. For the analysis of time course accumulation, a human colon adenocarcinoma cell line, COLO206, was used. As showed in Figure 8, gemini **1** noticeably increased the content of the photosensitizer in COLO206 cells. In particular, both DMPC/**1** 7:3 and 8:2 proved to be the more efficient formulations for the uptake of *m*-THPC by the cells.

LSCM observations carried out on living COLO206 cells confirmed flow cytometry results. In fact, COLO206 cells treated with *m*-THPC in DMPC liposomes for 1 h displayed a very low fluorescent signal (Figure 9a), when compared to cells treated with *m*-THPC in DMPC/**1** 7:3 (Figure 9b) and DMPC/**1** 8:2 liposomes (Figure 9c). The analysis of optical sections allowed us to demonstrate that in cells treated with the two formulations a great amount of photosensitizer was localized in the plasma membrane, whereas fluorescence was scarcely detectable in the cytoplasm. After 4 h, in samples treated with *m*-THPC DMPC/**1** 7:3 the fluorescence was also detectable in the cytoplasm of COLO206 cells. (Figure 9d). A similar distribution was detectable in *m*-THPC DMPC/**1** 8:2-treated samples: in this case, the photosensitizer was shown to be localized also in the nuclei (Figure 9e)

3. Conclusions

The successful delivery of a drug to an organism depends on many parameters, so that is not wise to expect a simple and straightforward relationship between the efficiency of delivering and the physicochemical features of the vector. However, the above-discussed results demonstrate that it is possible, to some extent, to correlate the physicochemical and biological features of lipid drug vehicles. This possibility opens promising perspectives in the design of new formulations. It is clear from the reported biological evaluation that the mixed DMPC/**1** liposomes are, in a determinate range of component molar ratios, more efficient in delivery with respect to DMPC liposomes, due to a favorable interaction of the cationic components with the cell membrane. The favorable interaction with the membrane counterbalances the minor amount of PS entrapped in the liposomes as a consequence of the addition of gemini to the formulation. At a DMPC/**1** 6:4 molar ratio the efficiency of delivery drops abruptly in correspondence to a phase transition that was observed, in the characterization of the vectors, both in solution (DLS, fluorescence) and on solid support (TEM, EDXD).

The DLS measurements (Table 2) gave, in fact, for the formulations up to a 7:3 DMPC/**1** molar ratio the size expected on the basis of the extrusion protocol, whereas for the 6:4 formulation they evidenced a major population centered at 150 nm and a minor population that could be diagnostic of the emergence of a new anisotropic phase. In the investigation on the phase transition temperature of the liposomes, carried out by Laurdan fluorescence experiments, we observed that the linear increase of the transition temperature as a function of the increase of gemini content drops in correspondence of the 6:4 dispersion. In the investigation of fluorescence-quenching experiments of the entrapped PS by iodide or methyl viologen, the PS that resulted was completely protected from the quencher by the 6:4 DMPC/**1** formulation, whereas it was completely accessible to quencher in pure DMPC liposomes and partially accessible in the other tested formulations (Figures 3 and 4). The presence of two populations (one reachable and one unreachable by the quenchers) in the 8:2 and 7:3 DMPC/**1** dispersions suggests a partition of the PS in different domains of the lipid double layer.

The phase transition corresponding to the 40% gemini formulation was observed not only by the different standpoints of investigation in solution, but also by the TEM and EDXD investigations carried out on dehydrated samples. In general, a comparison of the results obtained in completely different experimental conditions has to be made cautiously; however, both techniques show that at a DMPC/**1** ratio of 6:4 the mixed system undergo a phase transition. The different conditions of the investigated samples imply the observation, in the TEM images (Figure 2b,c), of multilamellar fused systems in contrast with the 100 nm liposomes observed by DLS (as expected according to the freeze−thaw protocol). Conversely, EDXD experiments, though carried out on dehydrated sample, besides evidencing the phase transition, confirm the presence of lipid domains suggested by the fluorescence quenching experiments carried out in solution. Furthermore, the results relative to the EDXD experiments suggest that the PS is located differently in the dispersions up to a 7:3 DMPC/**1** ratio and in the 6:4 formulation. In particular, it should be positioned in the region of the headgroups in the 8:2

and 7:3 formulations and embedded in the hydrophobic region of the double layers in the 6:4 aggregates, as shown also by the results obtained in the fluorescence quenching experiments.

The work carried out demonstrates that by combining different tools it is possible to gain a quite complete description of the microscopic organization of lipid aggregates and of their complexes with a drug. Some of the morphological and physicochemical features of the systems can be related to their biological behavior. This possibility opens new perspectives toward a rational and systematic approach to the design of liposomes as drug vehicles.

4. Experimental Section

4.1. Materials. Dimyristoyl-*sn-glycero*-phosphatidylcoline (DMPC) was purchased from Avanti Polar Lipids (Alabaster, AL), Laurdan (6-dodecanoyldimethylaminonaphthalene) from Fluka, and exclusion gel Bio-Gel A-15 m gel from Bio-Rad Laboratories (Hercules, CA); *m*-tetrahydroxyphenylchlorin (*m*-THPC) was a kind gift from Prof. Thierry Patrice, Université de Nantes, France. RPE- and HPLC-grade solvents (chloroform, ethanol, 2-propanol, bidistilled water) were purchased from Carlo Erba Reagenti (Milano, Italy).

NMR spectra were collected on a Bruker AC 300 P spectrometer operating at 300.13 and 75.47 MHz for ^{1}H and ^{13}C, respectively, equipped with a sample tube thermostating apparatus. Signals were references with respect to TMS (δ = 0.000 ppm) used as an internal standard in $CDCl_3$ and CD_3OD. Steady-state fluorescence experiments were carried out, unless otherwise specified, on a Shimadzu RF5001PC spectrofluorimeter. Spectrofotometric experiments were carried out on a Varian Cary 300 Bio. Melting points were determined with a Barnstead-thermolyne instrument and are uncorrected. Optical rotation measurements were carried out on a Perkin-Elmer-241 polarimeter using a cell of 10 cm path length.

4.2. Preparation of Gemini Surfactant 1. To 0.2 g (1 mmol) of (2*S*,3*S*)-2,3-dimetoxy-1,4-bis(*N*,*N*-dimethylamine)-butane[27] in benzene was added 1.2 mL of bromohexadecane (3.9 mmol) and the solution was kept at room temperature. After 20 days the formation of a white precipitate was observed. The reaction mixture was filtered; the precipitate was washed many times with diethyl ether and crystallized from acetone (yield 60%): mp 408 K (dec); ^{1}H NMR, (δ $CDCl_3$);^{13}C NMR, (δ $CDCl_3$); α_D −20° (c = 3, $EtOH_{abs}$); ES-MS $[735]^+$ (monocation). Anal. ($C_{42}H_{90}N_2O_2Br_2 \cdot 1.5H_2O$) C, H, N.

4.3. Liposome Preparation. The aqueous dispersions of DMPC/**1** liposomes were prepared according to the procedure described by Hope et al.[28] A film of lipid (total 20.0 μmol) was prepared on the inside wall of a round-bottom flask by evaporation of $CHCl_3$ solutions containing the proper amount of DMPC and **1** to obtain the molar percentage mixture. The obtained films were stored in a desiccator overnight under reduced pressure and to them were added 1 mL of PBS buffer solution (Aldrich, 10^{-2} M pH 7.4) in order to obtain a 12.5 mM lipid dispersion. The solutions were vortex-mixed and then freeze−thawed six times from liquid nitrogen to 313 K. Dispersions were then extruded (10 times) through a 100 nm polycarbonate membrane (Whatman Nucleopore). The extrusions were carried out at 307 K, well above the transition temperature of DMPC (297.2 K), using a 2.5 mL extruder (Lipex Biomembranes, Vancouver, Canada). *m*-THPC-containing liposomes were prepared by adding to the chloroform solution of the lipids the proper volume of a *m*-THPC stock solution (5×10^{-4} M, absolute EtOH) to obtain, after hydration, a final concentration of 50 μmol *m*-THPC.

4.4. Determination of Entrapped Drug Percentage. Nonentrapped drug was separated by filtration of 200 μL of liposome solution on a 2.5 mL Bio-Rad AM-15 gel column, equilibrated in PBS buffer solution. Fractions containing liposomes were identified by fluorescence emission of *m*-THPC and then combined and diluted to a known volume. *m*-THPC concentration in liposome preparations before and after filtration was determined by measuring the absorbance maximum (at 652 nm) of the *m*-THPC/liposomes disrupted by the addition of an equal volume of 2-propanol, the molar extinction coefficient of the free *m*-THPC in 50% 2-propanol/water being 158 600. The percentage of entrapped drug was calculated using the equation[29]

$$\%\ m\text{-THPC} = 100 \times (M^{a}_{m-\mathrm{THPC}} M^{b}_{\mathrm{lip}})/(M^{b}_{m-\mathrm{THPC}} M^{a}_{\mathrm{lip}}) \quad (2)$$

where $M^{a}_{m-\mathrm{THPC}}$ and $M^{b}_{m-\mathrm{THPC}}$ are the chlorin concentration in liposomes, respectively, after and before gel filtration and M^{a}_{lip} and M^{b}_{lip} are the total lipid concentration after and before the filtration, respectively.

4.5. Determination of Total Lipid Concentration (M^{a}_{lip} and M^{b}_{lip}). Total lipid (DMPC + **1**) concentration in liposomes dispersions before and after filtration was determined by ^{1}H NMR. Liposome preparations before and after gel filtration were analyzed in the presence of an internal standard, tris-(2,2′-bipyridyl) ruthenium(II)hexahydrate chloride, according to the following procedure. A known volume of liposome solution was dried under vacuum, the residue was dissolved in a known volume of CD_3OD and then to it was added the proper amount of the CD_3OD standard solution to obtain a 2.5 mM nominal lipid concentration and a 0.7 mM standard concentration. ([standard] = 28.2% [lipids]). As reference signals for integration, with respect to the standard aromatic signals, we chose the signals at 2.3 ppm (4H) and 1.8 ppm (4H) DMPC and **1**, respectively (Chart 1).

4.6. Determination of Liposome Phase Transition Temperature as a Function of the Percentage of 1. Liposome phase transition temperature was determined by a spectrofluorimetric method[30] using Laurdan as fluorescent probe. A mixed film was prepared from a chloroform solution containing a weighted amount of lipids (DMPC + **1**) and a volume of a Laurdan 2 mM chloroform stock solution to obtain a 60 μM Laurdan concentration and a 12.5 mM lipid concentration (molar ratio lipid/Laurdan = 200). Liposomes solutions were prepared as described in section 2.2. For emission measurements, liposome dispersions were diluted with PBS buffer in order to obtain a 0.4 μM Laurdan concentration. Temperature was controlled by a circulating bath and the actual temperature was measured in the sample cuvette by a thermocouple. Emission spectra (λ_{ecc} = 350 nm) were acquired as a function of temperature, at intervals of 1 K, in the range 286−318 K. The generalized polarization parameter (GP)[30] was calculated for each liposome preparation by eq 3

$$\mathrm{GP} = (I_B - I_R)/(I_B + I_R) \quad (3)$$

where I_B (450 nm) and I_R (490 nm) are the fluorescence emission intensities corresponding to the emission maxima of Laurdan in the gel and in the liquid crystalline phase, respectively. The transition temperature for each liposome preparation corresponds to the inflection point in the GP versus temperature plots.

4.7. Morphological Analysis by Transmission Electron Microscopy (TEM). Samples for TEM experiments was prepared as follows: a droplet of each liposome solution, prepared as described in section 2.3, was deposited onto a 300 mesh copper grid for electron microscopy, covered with a thin (about 20 nm) amorphous carbon film. The excess of solution was removed by placing the grid on filter paper. A droplet of stain solution (phosphotungstate acid aqueous solution 2% w/v buffered at pH = 7.40 with NaOH) was then added and the excess of solution removed.

The samples were studied in a Zeiss 902 TEM, operating at 80 kV. To enhance the contrast, the microscope was settled with electron energy loss imaging filter. The filter was settled to collect only elastic electrons (ΔE = 0), to avoid the contribution of inelastic electrons to the contrast formation. Inelastic electrons scattered from the sample contribute only to the image background noise and their filtering out strongly enhances the final image quality.[31]

4.8. Morphological Analysis by Dynamic Light Scattering (DLS). Light scattering measurements were made by using ca. 1 mL of sample in 6 mm diameter Pyrex glass culture tubes, protected from dust by Parafilm caps. The cylindrical glass sample tube was fixed at the center of a toluene-filled fluorimeter cuvette to provide refractive index matching against stray light reflections. The cuvette was housed in a black-anodized aluminum cell block, whose temperature was regulated by a Peltier thermoelectric element. The light source was a Coherent Innova 70-3 argon-ion laser operating at 4880 Å. Light scattered at 90° was collected from approximately one coherence area and imaged onto the slit of a photomultiplier tube (Products for Research, Inc.). A 64-channel Nicomp Model 370 computing autocorrelator was used to calculate and display the diffusion coefficient, D, and the associated parameters derived from cumulants analysis[32] and nonlinear least squares (NLLS) fits (method of inverse Laplace transform, ILT[33]) to the intensity autocorrelation function. All measurements showed reasonable goodness-of-fit values. The hydrodynamic radii, R_h, can be estimated by applying the Stokes–Einstein relation (for stick-boundary conditions)[21]

$$D = kT/6\pi\eta R_h \quad (4)$$

where η is the viscosity of the solution, which can be approximated to that of water.

4.9 Fluorescence Experiments. Steady-state fluorescence experiments were carried out on a SPEX-Fluoromax spectrofluorimeter (Edison, NJ), operating in single photon counting (SPC) acquisition mode. All fluorescence experiments were carried out on solutions with optical densities lower than 0.05 to minimize inner filter effects. Fluorescence quenching experiments were performed at 15 °C by adding small aliquots of 2 M iodide or 1 M methyl viologen solutions to the liposome formulations, previously filtered on a gel column (see section 2.4), diluted in order to obtain [*m*-THPC] = 0.75 μM. The obtained solutions were incubated for 15 min. Time-resolved fluorescence experiments were performed on a CD900 fluorimeter with SPC detection (Edinburgh Instruments). Excitation was achieved by an arc lamp filled with ultrapure hydrogen gas (pressure 0.030 bar; repetition rate 40 kHz; full width half-maximum = 1.2 ns). Experimental time decays were deconvoluted by a nonlinear least-squares analysis to multiexponential functions by using standard software licensed by Edinburgh Instruments. Fluorescence anisotropy measurements were performed on the SPEX apparatus, equipped with Glan-Thomson polarizing prisms. The steady-state anisotropy coefficient is defined as $r = (I_{||} - I_{\perp})/(I_{||} + 2I_{\perp})$, where $I_{||}$ and $I_{\perp}$ are the fluorescence intensities measured with the emission polarizer set parallel or perpendicular to the excitation polarization direction, respectively. r_0 represents the anisotropy coefficient for a chromophore, whose rotational motion is completely hindered ($r_0 = 0.11 \pm 0.01$).[22] In all fluorescence experiments stray-light contamination was minimized by using a cutoff filter at 600 nm (LOT-Oriel, Italy).

4.10. Energy Dispersive X-ray Diffraction (EDXD). X-ray diffraction experiments were carried out by using an energy-dispersive X-ray diffraction (EDXD) apparatus described elsewhere.[34] The diffractometer operates in vertical θ/θ geometry and is equipped with an X-ray generator (W target), a collimating system, step motors, and a solid-state detector connected via an electronic chain to a multichannel analyzer. The X-ray source is a standard Seifert tube operating at 50 kV and 40 mA whose continuous Bremsstrahlung radiation is used; the detecting system is composed of an EG&G liquid nitrogen cooled ultrapure Ge solid-state detector connected to a PC through ADCAM hardware. Both the X-ray tube and the detector can rotate around their common center, where a cell is placed. After a preliminary set of measurements, one scattering angle, $\theta = 0.35°$, was selected to investigate the range of interest of the reciprocal space. The uncertainty associated with θ is $\Delta\theta = 0.001°$ and it directly affects the uncertainty Δq associated with the transfer momentum q (q = cost E sin θ; cost = 1.01354 Å^{-1} keV^{-1}). Each EDXD scan was collected for t = 1000 s, and during such period no structural modification or damage of the samples occurs, as elsewhere discussed.[25]

4.11. Cell Cultures. The established human colon tumor cell line COLO206 (kindly provided by Dr. L. Rivoltini, Istituto Nazionale dei Tumori, Milano, Italy) were grown as monolayers in RPMI 1640 medium (Gibco Life Technologies, Paisley, UK) supplemented with 10% FBS (Hyclone, Carmlington, UK), 1% penicillin (50 U/mL), and streptomycin (50 μg/mL) (Gibco) in a humidified atmosphere of 5% CO_2 in a water-jacketed incubator at 37 °C.

4.12. Flow Cytometry. The time course analysis of liposome/*m*-THPC uptake was performed on COLO206 cells treated with five different liposome formulations, 1:100 diluted in culture medium (DMPC/**1**, *m*-THPC in DMPC, *m*-THPC in DMPC/**1** 8:2, *m*-THPC in DMPC/**1** 7:3, *m*-THPC in DMPC/1 6:4) for 30 min, 1 h, and 4 h. At the end of each treatment, cells were washed with ice-cold Hank's balanced salt solution (HBSS, Sigma), detached with EDTA and trypsin, resuspended in ice-cold PBS, and immediately analyzed for the photosensitizer content.

Fluorescence signals were analyzed with a FACScan flow cytometer (Becton Dickinson, Mountain View, CA) equipped with a 15-mW, 488-nm, air-cooled argon ion laser. The fluorescence emission was collected through a 670-nm bandpass filter and acquired in log mode, taking into account that fluorescence emission of *m*-THPC features two peaks at 650 and 714 nm, the more intense occurring at 650 nm.[35] At least 10 000 events were analyzed. The photosensitizer content was evaluated as fluorescence intensity and expressed in arbitrary units (AU), calculated as the ratio between the mean fluorescence channel (MFC) of treated samples versus the MFC of untreated cells. The analysis was performed by the CellQuest software (Becton Dickinson).

4.13. Laser Scanning Confocal Microscopy. Living cells were analyzed by laser scanning confocal microscopy (LSCM) in order to investigate the intracellular distribution of the different liposome formulations. Cells, grown on 12 mm glass coverslips, were inoculated with the different liposome formulations, under stirring at 300 rpm. After an incubation of 1 and 4 h at 37 °C, cells were fixed in 3.7% paraformaldehyde in PBS, for 10 min at room temperature. Observations were performed by using a Leica TCS 4D laser scanning confocal microscopy (Leica, Microsystems, Mannheim, Germany) equipped with an Ar/Kr laser. After excitation at 568 nm, fluorescence emission was collected using a 590 nm long-pass filter.

Acknowledgment. We gratefully acknowledge MIUR financial contribution for the FIRB project "Preparation and characterization of liposomes as biomembrane models and drug carriers in photodynamic therapy". G.C. is grateful to MIUR (Cofin 2003038084) for financial support.

Supporting Information Available: ^{1}H NMR and ^{13}C NMR characterization and elemental analysis values for compound **1**. This material available free of charge via the Internet at http://pubs.acs.org.

References

(1) Bangham, A. D.; Standish, M. M.; Watkins, J. C. Diffusion of univalent ions across the lamellae of swollen phospholipids. *J. Mol. Biol.* **1965** *13*, 238–252.
(2) (a) Papahadjopoulos, D., Ed. Liposomes and Their Uses in Biology and Medicine. *Ann. N.Y. Acad. Sci.* **1978**, *308*. (b) *Liposomes, from Physical Structure to Therapeutic Applications*; Knight, C. G.; Ed.; Elsevier/North-Holland: Amsterdam, 1981. (c) *Liposomes from Biophysics to Therapeutics*; Ostro, M. J.; Ed; Marcel Dekker: New York, 1987. (d) *Liposomes as Drug Carriers: Recent Trends and Progress;* Gregoriadis, G.; Ed.; John Wiley & Sons: New York, 1988.
(3) Lasic, D. D. Liposomes in Drug Delivery. In *Vesicles*; Rosoff, M.; Ed.; Marcel Dekker: New York, 1996; pp 447–476.
(4) Lasic, D. D. *Liposomes: From Physics to Applications;* Elsevier: Amsterdam, 1993.

(5) Konan, Y. N.; Gurny, R.; Allémann, E. State of the art in the delivery of photosensitizers for photodynamic therapy. *J. Photochem. Photobiol. B: Biol.* **2002**, *66*, 89−106.
(6) Keene, J. P.; Kessel, D.; Land, E. J.; Redmond, R. W.; Truscott, T. G. Direct detection of singlet oxygen sensitized by haematoporphyrin and related compounds. *Photochem. Photobiol.* **1986**, *43*, 117−120.
(7) Damoiseau, X.; Schuitmaker, H. J.; Lagerberg, J. W.; Hoebeke, M. Increase of the photosensitizing efficiency of the Bacteriochlorin a by liposome-incorporation. *J. Photochem. Photobiol. B: Biol.* **2001**, *60*, 50−60.
(8) a) Milanesi, C.; Sorgato, F.; Jori, G. Photokinetic and ultrastructural studies on porphyrin photosensitization of HeLa cells. *J. Radiat. Biol.* **1989**, *55*, 59−69. (b) Ricchelli, F.; Gobbo, S.; Jori, G.; Moreno, G.; Vinzens, F.; Salet, C. Photosensitization of mitochondria by liposome-bound porphyrins. *Photochem. Photobiol.* **1993**, *58*, 53−58.
(9) Derycke, A. S. L.; de Witte, P. A. M. Liposomes for photodynamic therapy. *Adv. Drug Delivery Rev.* **2004**, *56*, 17−30.
(10) a)Pires, P.; Simoes, S.; Nir, S.; Gaspar, R.; Duzgunes, N.; Pedroso de Lima, M. C. Interaction of cationic liposomes and their DNA complexes with monocytic leukemia cells. *Biochim. Biophys. Acta* **1999**, *1418*, 71−84. (b) Felgner, P. L.; Ringold, G. M. Cationic liposome-mediated transfection. *Nature* **1989**, *337*, 387−388.
(11) Senior, J. H.; Trimble, K. R.; Maskievicz, R. Interaction of positively charged liposomes with blood: Implications for their application in vivo. *Biochim. Biophys. Acta* **1991**, *1070*, 173−179.
(12) Menger, F. M.; Keiper, J. S. Gemini surfactants. *Angew. Chem., Int. Ed.* **2000**, *39*, 1906−1920.
(13) (a) McGregor, C.; Perrin, C.; Monck, M.; Camilleri, P.; Kirby A. J. Rational approaches to the design of cationic gemini surfactants for gene delivery. *J. Am. Chem. Soc.* **2001**, *123*, 6215−6220. (b) Fielden, M. L.; Perrin, C.; Kremer, A.; Bergsma, M.; Stuart, M. C.; Camilleri, P.; Engberts J. B. F. N. Sugar-based tertiary amino gemini surfactants with a vesicle-to-micelle transition in the endosomal pH range mediate efficient transfection in vitro. *Eur. J. Biochem.* **2001**, *268*, 1269−1279.
(14) (a) Sumida, Y.; Masuyama, A.; Takasu, M.; Kida, T.; Nakatsuji, Y.; Ikeda, I.; Nojima, M. Behavior of self-organized molecular assemblies composed of hosphatidylcholines and synthetic triple-chain amphiphiles in water. *Langmuir* **2000**, *16*, 8005−8009. (b) Sumida, Y.; Masuyama, A.; Takasu, M.; Kida, T.; Nakatsuji, Y.; Ikeda, I.; Nojima, M. New pH-sensitive vesicles. Release control of trapped materials from the inner aqueous phase of vesicles made from triple-chain amphiphiles bearing two carboxylate groups. *Langmuir* **2001**, *17*, 609−612.
(15) C. Hadjur, N. Lange, J. Rebstein, P. Monnier, H. van den Bergh, G. Wagnières Spectroscopic studies of photobleaching and photoproduct formation of meta(tetrahydroxyphenyl)chlorin (m-THPC) used in photodynamic therapy. The production of singlet oxygen by m-THPC. *J. Photochem. Photobiol. B: Biol.* **1998**, *45*, 170−178.
(16) Peng, Q.; Moan, J.; Ma, L. W.; Nesland, J. M. Uptake, localization and photodynamic effect of *meso*-tetra-(hydroxyphenyl)-porphirine and its corresponding chlorin in normal and tumor tissues of mice bearing mammary carcinoma. *Cancer Res.* **1995**, *12*, 2620−2626.
(17) Chen, Y.; Xu, S.; Li, L.; Zhang, M.; Shen, J.; Shen, T. Active oxygen generation and photooxygenation involving temporfin (m-THPC). *Dyes Pigments* **2001**, *51*, 63−69.
(18) Semple, T. U.; Quinn, L. A.; Woods, L. K.; Moore, G. E. Tumor and lymphoid cell lines from a patient with carcinoma of the colon for a cytotoxicity model. *Cancer Res.* **1978**, *38*, *8* (5), 1345−1355.
(19) Sujatha, J.; Mishra, A. K. Phase transitions in phospholipid vesicles: Excited-state prototropism of 1-naphthol as a novel probe concept. *Langmuir* **1998**, *14*, 2256−2262.
(20) Valentine, R. C.; Shapiro, B. M.; Stadtman, E. R. Regulation of glutamine synthetase. XI. The nature and implications of a lag phase in the *Escherichia coli* glutamine synthetase reaction. *Biochemistry* **1968**, *7* (6), 2136−2142.
(21) Berne, B. J.; Pecora, R. *Dynamic Light Scattering with Applications to Chemistry, Biology and Physics*; Wiley: New York, 1976.
(22) Maiti, N. C.; Mazumdar, S.; Periasamy, N. Dynamics of porphyrin molecules in micelles. Picosecond time-resolved fluorescence anisotropy studies. *J. Phys. Chem.* **1995**, *99*, 10708−10715.
(23) Caracciolo, G.; Mancini, G.; Bombelli, C.; Caminiti, R. Structural features of a cationic gemini surfactant at full hydration investigated by energy-dispersive X-ray diffraction. *Chem. Phys. Lett.* **2004**, *386* (1−3), 76−82.
(24) Wiehe, A.; Simonenko, E. J.; Senge, M. O.; Röder, B. Hydrophilicity vs hydrophobicity—Varying the amphiphilic structure of porphyrins related to the photosensitizer m-THPC. *J. Porph. Phthal.* **2001**, *5* (10), 758−761.
(25) Caracciolo, G.; Amiconi, G.; Bencivenni, L.; Boumis, G.; Caminiti, R.; Finocchiaro, E.; Maras, B.; Paolinelli, C.; Congiu Castellano, A. Conformational study of proteins by SAXS and EDXD: The case of trypsin and trypsinogen. *Eur. Biophys. J.* **2001**, *30*, 163−170.
(26) Zumbuehl, O.; Weder, H. G. Liposomes of controllable size in the range of 40 to 180 nm by defined dialysis of lipid/detergent mixed micelles. *Biochim. Biophys. Acta* **1981**, *640*, 252−262.
(27) Seebach, D.; Kalinowski, H. O.; Bastani, B.; Crass, G.; Daum, H.; Dorr, H.; DuPreez, N. P.; Ehrig, V.; Langer, W.; Nussler, C.; Oei, Hoc-An; Schmidt, M. Preparation of auxiliaries for asymmetric synthesis from tartaric acid. Additions of butyllithium to aldehydes in chiral media. *Helv. Chim. Acta* **1977**, *60* (2), 301−325.
(28) Hope, M. J.; Nayar, R.; Mayer, L. D.; Cullis, P. R. Reduction of liposomes size and preparation of unilamellar vesicles by extrusion techniques. In *Liposome Technology,* 2nd ed.; Gregoriadis, G.; Ed.; CRC Press: Boca Raton, FL, 1992; Vol. I, pp 123−139.
(29) Hwang; S H.; Maitani, Y.; Qi, X R.; Takayama, K.; Nagai, T. Remote loading of diclofenac, insulin and fluorescein isothiocyanate labeled insulin into liposomes by pH and acetate gradient methods. *Int. J. Pharm.* **1999**, *179*, 85−95.
(30) Parasassi, T.; De Stasio, G.; D′Ubaldo, A.; Gratton, E. Phase fluctuation in phospholipid membranes revealed by Laurdan fluorescence. *Biophys. J.* **1990**, *57*, 1179−1186.
(31) Egerton, R. F. *Electron energy loss spectroscopy*; Plenum Press: New York, 1986.
(32) Koppel, D. E. Analysis of macromolecular polydispersity in intensity correlation spectroscopy. Method of cumulants. *J. Chem. Phys*, **1972**, *57* (11), 4814−4820.
(33) Provencher, S.; Hendrix, J.; De Maeyer, L.; Paulussen, N. Direct determination of molecular weight distributions of polystyrene in cyclohexane with photon correlation spectroscopy. *J. Chem. Phys*. **1978**, *69*, 4273−4276.
(34) Caminiti, R.; Rossi Albertini, V. The kinetics of phase transitions observed by energy-dispersive X-ray diffraction. *Int. Rev. Phys. Chem*. **1999**, *18* (2), 263−299.
(35) Bourre, L.; Thibaut, S.; Briffaud, A.; Rousset, N.; Eleouet, S.; Lajat, Y.; Patrice, T. Indirect detection of photosensitizer ex vivo. *J. Photochem. Photobiol. B: Biol*. **2002**, *67*, 23−31.

JM050182D